Exploring the behaviour of luminescence signals from feldspars

Colarossi, Debra; Duller, G. A. T.; Roberts, H. M.

Published in:
Radiation Measurements

DOI:
10.1016/j.radmeas.2017.07.005

Publication date:
2018

Citation for published version (APA):
Colarossi, D., Duller, G. A. T., & Roberts, H. M. (2018). Exploring the behaviour of luminescence signals from feldspars: Implications for the single aliquot regenerative dose protocol. *Radiation Measurements*, *109*, 35-44. https://doi.org/10.1016/j.radmeas.2017.07.005

Radiation Measurements 109 (2018) 35–44

Contents lists available at ScienceDirect

Radiation Measurements

journal homepage: www.elsevier.com/locate/radmeas

Exploring the behaviour of luminescence signals from feldspars: Implications for the single aliquot regenerative dose protocol

D. Colarossi*, [1], G.A.T. Duller, H.M. Roberts

Department of Geography and Earth Sciences, Aberystwyth University, Ceredigion SY23 3DB, UK

HIGHLIGHTS

- Successful dose recovery for post-IR IRSL signal using SAR is test dose dependent.
- Difficulty of IRSL signal removal causes carry-over of charge during SAR protocol.
- Increasing test dose size or stimulation time reduces apparent sensitivity change.
- Single grain D_e overdispersion value is influenced by test dose size.
- A new method is proposed to minimise carry-over of charge between L_x and T_x.

ARTICLE INFO

Article history:
Received 10 January 2017
Received in revised form
19 May 2017
Accepted 19 July 2017
Available online 20 July 2017

Keywords:
SAR
Luminescence dating
Single grain
Post-IR IRSL signal
Dose recovery
Test dose

ABSTRACT

A series of dose recovery experiments are undertaken on grains of potassium-rich feldspar using a single aliquot regenerative dose (SAR) protocol, measuring the post-infrared infrared stimulated luminescence (post-IR IRSL) signal. The ability to successfully recover a laboratory dose depends upon the size of the test dose used. It is shown that using current SAR protocols, the magnitude of the luminescence response (T_x) to the test dose is dependent upon the size of the luminescence signal (L_x) from the prior regeneration dose because the post-IR IRSL signal is not reduced to a low level at the end of measuring L_x. Charge originating from the regeneration dose is carried over into measurement of T_x. When the test dose is small (i.e. 1%–15% of the given dose) this carry-over of charge dominates the signal arising from the test dose. In such situations, T_x is not an accurate measure of sensitivity change. Unfortunately, because the carry-over of charge is so tightly coupled to the size of the signal arising from the regeneration dose, standard tests such as recycling will not identify this failure of the sensitivity correction. The carry-over of charge is due to the difficulty of removing the post-IR IRSL signal from feldspars during measurement, and is in stark contrast with the fast component of the optically stimulated luminescence (OSL) signal from quartz for which the SAR protocol was originally designed.

1. Introduction

A series of papers in the last 8 years has revolutionised the potential for using feldspars in luminescence dating (e.g. Thomsen et al., 2008; Li and Li, 2011; Jain and Ankjærgaard, 2011; Buylaert et al., 2012; Li et al., 2014). The post-infrared infrared stimulated luminescence (post-IR IRSL) method (Thomsen et al., 2008; Buylaert et al., 2012), and the multiple elevated temperature (MET) method (Li and Li, 2011), provide approaches for obtaining luminescence signals that are far less prone to anomalous fading (Wintle, 1973) than those measured close to room temperature. When this new signal is combined with the single aliquot regenerative dose (SAR) method originally designed for quartz (Murray and Wintle, 2000), it provides an exciting new approach for luminescence dating, and these innovations have been rapidly adopted at both the multiple grain and single grain level (e.g. Kars et al., 2014; Reimann et al., 2012).

However, a continuing area of uncertainty in the use of the SAR procedure for feldspars has been the role that changes in test dose have upon results. In a recent paper, Yi et al. (2016) provide a detailed experimental data set demonstrating the impact of changes in test dose upon the ability to recover a known laboratory

* Corresponding author.
E-mail address: debra_colarossi@eva.mpg.de (D. Colarossi).
[1] Current address: Department of Human Evolution, Max Planck Institute for Evolutionary Anthropology, Deutscher Platz 6, 04103 Leipzig, Germany.

http://dx.doi.org/10.1016/j.radmeas.2017.07.005

dose, and upon the equivalent dose (D_e) obtained. In their study on the post-IR $IRSL_{290}$ signal from density-separated 63–90 μm feldspar from Chinese loess, they demonstrated that the dose recovery ratio varies systematically with test dose (their Fig. 4(a)); an overestimated dose recovery is seen when a test dose of less than 15% of the given dose is used, and an underestimate is seen when the test dose is more than 80% of the given dose, and there is no sign of a plateau in the data. A similar pattern is seen for the assessment of D_e (their Fig. 5), though here the range of acceptable test doses is narrower, between 20 and 60% of the D_e, and in the absence of independent age control it is difficult to be certain whether the D_e values obtained with this range of test dose are accurate. The observation that the outcome of these critical experiments is dependent upon the size of the test dose is not new (e.g. Qin and Zhou, 2012; and see review by Li et al., 2014), but it is unsatisfactory both for practical and epistemological reasons. Practically, it means that an iterative approach is often needed when applying the SAR protocol to feldspars, with an initial set of measurements needed to gain an approximate value for D_e so that the correct size of the test dose can be calculated, and then a second set of measurements made in which this test dose is applied. For measurements of samples where the D_e may vary between different grains (e.g. incompletely bleached samples, Colarossi et al., 2015) the choice of an appropriate test dose is challenging, or impossible. From an epistemological point of view, the lack of any clear understanding of why the SAR protocol applied to feldspars is so sensitive to the choice of test dose is unsatisfactory, and inhibits the development of new methods which are less sensitive to the choice of test dose.

Whilst Yi et al. (2016) and others have provided clear evidence that accurate dose recovery depends upon the choice of test dose, and that using a large test dose is generally more successful than using a small test dose, there has not been a clear exploration of why a large test dose helps, and what this implies for the application of the SAR procedure to feldspars. This paper reports a series of dose recovery experiments, first keeping the size of the test dose constant and varying the size of the dose to be recovered, and second keeping the dose to be recovered constant and varying the size of the test dose. The data arising from these measurements are analysed to explore the changes that are occurring in the luminescence signals, and in the light of these results, significant challenges in the use of the SAR procedure with feldspars are discussed, as well as methods for minimising these problems. The luminescence measurements have been undertaken using a single grain IRSL system, but the data are analysed and discussed both at an aliquot level (by mathematically combining the signal from all 100 grains on an aliquot) to look for general trends, and at a single grain level to explore the variability.

2. Samples, instruments and measurement parameters

All experiments in this paper were undertaken on feldspar grains 180–212 μm in diameter, extracted from sample Aber162/MPT4, a late Quaternary fluvial deposit in South Africa, described by Colarossi et al. (2015). Potassium-rich feldspar was extracted through heavy liquid separation using sodium polytungstate at densities of 2.58 g cm^{-3} and 2.53 g cm^{-3} and the resulting material has a potassium concentration of 12.6 ± 0.8% determined using GM-beta counting. This value of K is close to the theoretical limit for feldspars (~14% by weight), and implies that the sample is predominantly composed of potassium-rich feldspar grains. The grains were not etched in hydrofluoric acid (HF) due to concerns about anisotropic removal of the surface (Duller, 1992).

Luminescence measurements were undertaken on an automated Risø TL/OSL-DA-15 reader. Simultaneous IR stimulation of all grains was undertaken using the IR LED array (875 nm, 146 mW cm^{-2}) and single grain stimulation was achieved with a focussed 150 mW IR laser (830 nm) mounted in the single grain OSL attachment (Bøtter-Jensen et al., 2003). Luminescence emitted in the blue region of the spectrum was detected by an EMI 9635Q PMT filtered by a combination of 2 mm BG-39 and 2 mm Corning 7–59 glass. Laboratory irradiations were made using a calibrated $^{90}Sr/^{90}Y$ beta source, with a dose rate of 0.0375 Gy s^{-1}. Unless stated otherwise, all measurements were made using the post-IR IRSL procedure shown in Table 1(a), based on Buylaert et al. (2009). The selection of an appropriate temperature at which to make post-IR IRSL measurements was outlined in Colarossi et al. (2015) where four post-IR IRSL signals were tested using stimulation temperatures of 225 °C, 250 °C, 270 °C and 290 °C. Similar recycling ratios, recuperation values, fading rates and dose recovery ratios were obtained at the four temperatures, and the post-IR $IRSL_{225}$ signal was selected because it produced the lowest residual dose, an important consideration for dating this relatively young sample. Anomalous fading is not expected to be an issue for the dose recovery experiments reported in this paper, because all measurements were made using the 'run one at a time' option to ensure a constant time between irradiation and IRSL measurement for each disc. For all dose recovery experiments reported in this paper, individual K-feldspar grains (180–212 μm) were mounted on single grain discs and bleached in a Honlë SOL-2 solar simulator for 48 h.

Data analysis was undertaken in Analyst V4.31 (Duller, 2015). Dose response curves were fitted with a single saturating exponential (SSE), double saturating exponential (DSE) or single exponential plus linear (SEPL) function, to obtain the "best fit" based on the reduced chi squared parameter. D_e values were determined by integrating the initial 0.165 s of the decay curve and subtracting the signal from a late background, taken from the last 0.33 s of the decay curve (Fig. 1). D_e values from individual grains were accepted

Table 1
Measurement protocols used during dose recovery experiments, steps in bold represent changes to the post-IR IRSL sequence shown in (a).

(a)

Step	Treatment	Measured
1	Beta irradiation	–
2	Preheat at 250 °C for 60 s	–
3	IRSL at 50 °C for 200 s (LEDs)	–
4	IRSL at 225 °C for 2 s (laser)	L_x
5	Beta irradiation	–
6	Preheat at 250 °C for 60 s	–
7	IRSL at 50 °C for 200 s (LEDs)	–
8	IRSL at 225 °C for 2 s (laser)	T_x
9	IRSL at 290 °C for 100 s (LEDs)	–

(b)

Step	Treatment	Measured
1	Beta irradiation	–
2	Preheat at 250 °C for 60 s	–
3	IRSL at 50 °C for 200 s (LEDs)	–
4	IRSL at 225 °C for 2 s (laser)	L_x
5	**IRSL at 225°C for 500 s (LEDs)**	–
6	Beta irradiation	–
7	Preheat at 250 °C for 60 s	–
8	IRSL at 50 °C for 200 s (LEDs)	–
9	IRSL at 225 °C for 2 s (laser)	T_x
10	**IRSL at 225°C for 500 s (LEDs)**	–

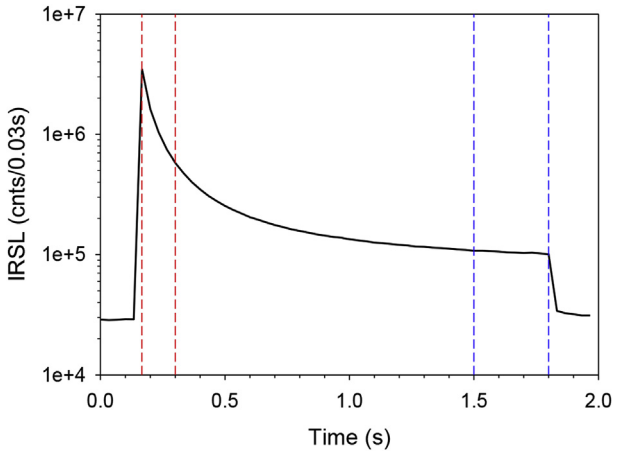

Fig. 1. Post-IR $IRSL_{225}$ decay curve measured using the IR laser during a 2 s stimulation. The signal is the sum of the signals from all 100 grains on one disc. The periods of time over which the data were summed to obtain the signal and the background are shown in red and blue, respectively. (For interpretation of the references to colour in this figure legend, the reader is referred to the web version of this article.)

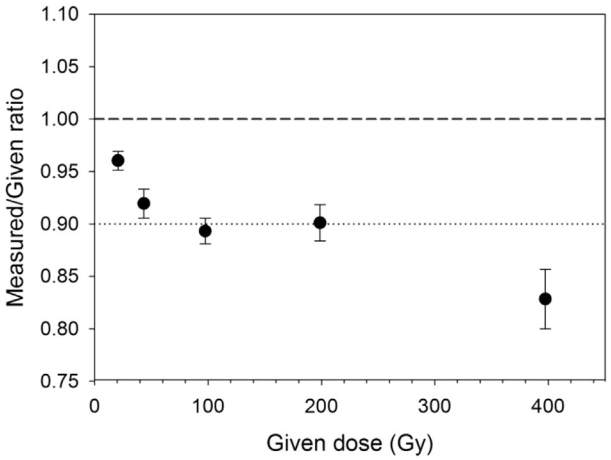

Fig. 2. Mean measured to given dose ratios from the post-IR $IRSL_{225}$ protocol (Table 1(a)) for given doses ranging between ~5 Gy and ~400 Gy with a fixed test dose of 5.1 Gy. The dotted line indicates the −10% lower limit for acceptance of the dose recovery test.

only if (i) the recycling ratio was within 10% of unity, (ii) recuperation was less than 5% of the largest regenerative dose, (iii) the error on the test dose signal was less than 3 standard deviations of the background signal, and (iv) the uncertainty on the test dose luminescence measurement was less than 10%.

3. Dose recovery of different given doses, using a fixed (5.1 Gy) test dose

Individual grains of K-feldspar were mounted on single grain discs, bleached for 48 h in the Honlë SOL-2 solar simulator and irradiated with a beta dose ranging between 21 Gy and ~400 Gy. Three discs were measured for each of the five given doses using the post-IR $IRSL_{225}$ protocol with a fixed test dose of 5.1 Gy. A high proportion of the single grains passed the acceptance criteria (between 48% and 73%) giving a statistically robust dataset of between 145 and 218 D_e values for each suite of experimental parameters.

Two single grain discs bleached in the SOL-2 received no laboratory dose and were used to determine the residual remaining within the grains after bleaching. For these residual measurements, the average D_e measured from the 135 grains which passed the screening criteria was 1.20 ± 0.08 Gy. This value was subtracted from the individual D_e values measured for all given doses. Mean measured to given dose ratios range from 0.96 ± 0.01 to 0.83 ± 0.03 (Fig. 2) and show a trend to increasingly poor dose recovery ratios as the size of the given dose increases. For the largest given dose (400 Gy) the dose recovery ratio (0.83 ± 0.03) is more than 10% from unity even allowing for the uncertainty, and thus the post-IR $IRSL_{225}$ protocol fails the dose recovery test when using a small test dose (5.1 Gy).

3.1. Single grain D_e distributions

The average values for the dose recovery ratio shown in Fig. 2 mask a number of important features of the single grain D_e measurements. To facilitate comparison of the shape of these distributions for the various given doses, individual D_e values were normalised to the relevant given dose and plotted as a histogram (Fig. 3) and radial plot (Fig. S1). At low given doses (20 Gy and 43 Gy) D_e distributions are slightly positively skewed and then become broader and more symmetrical as the given dose increases (Fig. 3). As well as becoming broader, the overdispersion (OD) increases with given dose (GD), from 9% (GD ~20 Gy) to 34% (GD ~400 Gy). The number of D_e values (n) in the distributions shown in Fig. 3 tends to decrease as the given dose increases. This is because an increasingly large number of grains that pass all of the screening criteria cannot be used to generate a D_e because they are saturated (n_{sat}, Fig. 3); that is to say that their normalised natural signal (L_n/T_n) is either at or above the maximum value from the SSE or DSE fit. Trauerstein et al. (2014) and Thomsen et al. (2016) suggest that a high number of saturated grains may bias the distribution towards lower D_e values and this is a plausible explanation of the systematic underestimation of the measured to given dose ratio observed in Fig. 2.

4. Dose recovery of a fixed (~400 Gy) given dose, using different test doses

A second experiment was undertaken, with bleached grains being irradiated with a given dose of ~400 Gy and the size of the test dose varied. The test doses applied were 5.1 Gy (~1% of the given dose), 20 Gy (~5%), 60 Gy (~15%), 120 Gy (~30%), 199 Gy (~50%) and 319 Gy (~80%), and were chosen to cover the range of values used in recent publications (e.g. 25% (Sohbati et al., 2012); 30% (Buylaert et al., 2013; Fu et al., 2015; Yi et al., 2015); 50% (Buylaert et al., 2015)). The dose recovery ratio obtained using a test dose of 5.1 Gy (0.83 ± 0.03) is the same data point as that shown in Fig. 2 (a given dose of 400 Gy). The measured to given dose ratio for the next highest test dose (20 Gy, ~5% of the given dose) jumps to 1.02 ± 0.02, and a steady decline in the ratio is then seen as the test dose increases to 199 Gy (~50%) (Fig. 4(a)). These results show it is possible to use the post-IR $IRSL_{225}$ signal to recover a large given dose (400 Gy), within 10% uncertainty, when a test dose of 5–80% of the given dose is applied. This is similar to the findings of Yi et al. (2016) for the post-IR $IRSL_{290}$ signal where a test dose of between 15% and 80% of the D_e is recommended.

4.1. Singe grain D_e distributions

The distributions of single grain D_e values at the two lowest test doses (5 Gy and 20 Gy; Fig. 5 and radial plots in Fig. S2) are broad and slightly positively skewed. The overdispersion (OD) drops rapidly as the test dose increases: 34% OD for a test dose of 5 Gy, 16% OD for a test dose of 20 Gy, and OD then becomes almost constant

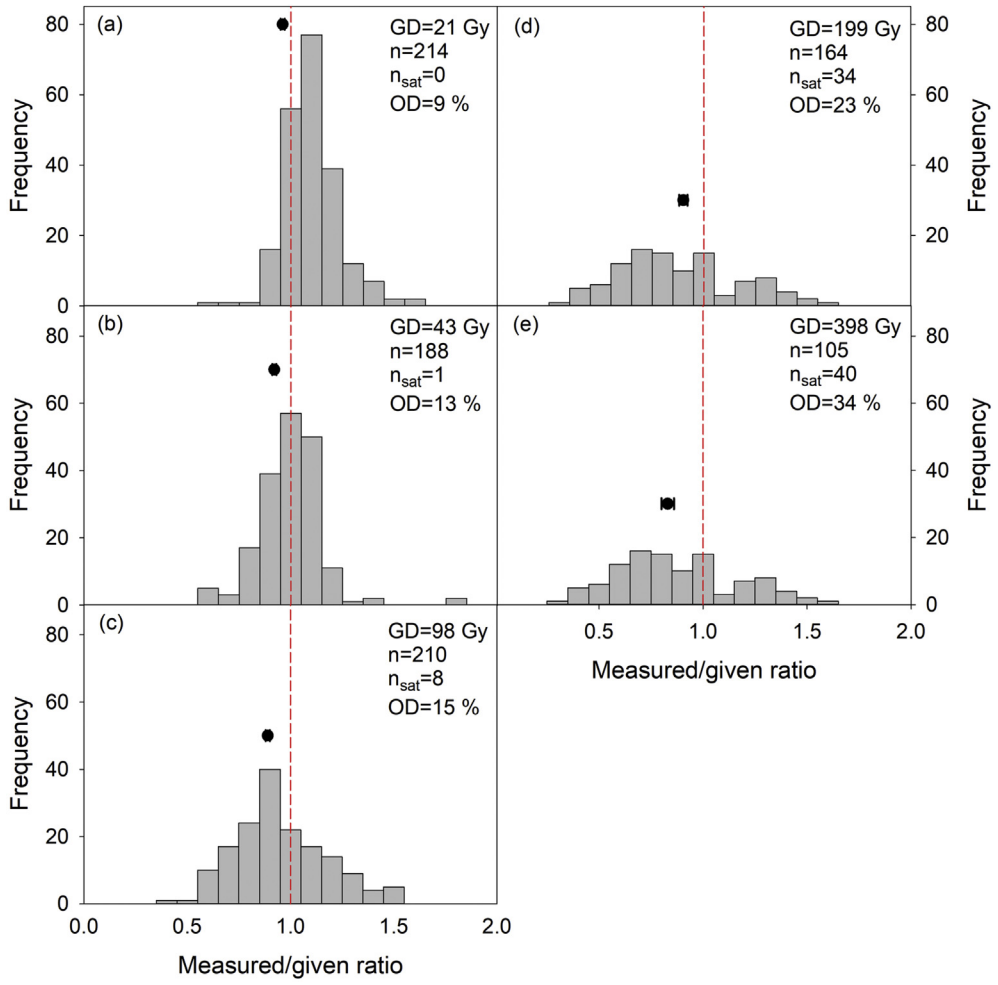

Fig. 3. The measured to given dose ratios for single grains of K-feldspar for the data shown in Fig. 2. The mean measured to given dose ratio for the distribution is denoted by the black dot shown with error bars (plotted against an arbitrary y-value). All measurements were made using the post-IR $IRSL_{225}$ protocol (Table 1(a)) with a fixed test dose of ~5.1 Gy; GD represents the given dose, n the number of grains included in the D_e distribution excluding the number of saturated grains (n_{sat}) and the dashed line indicates the given dose normalised to 1. Radial plots of these distributions are included in the supplementary information (Fig. S1).

at ~12% for higher test doses. Nian et al. (2012) observed a similar decrease in OD (~21%–14%) when increasing the size of their test dose from 25 Gy to 100 Gy.

The number of saturated grains observed for a fixed 400 Gy given dose decreases as the test dose increases (Fig. 5), from 40 grains for the 5.1 Gy test dose (1% of the given dose (GD)) to 3 grains at the ~320 Gy test dose (80% of GD). A range of test doses appear suitable, but there appears to be an optimum test dose between 15 and 30% of the given dose (60–120 Gy) where OD is low, the number of saturated grains is small, and the recovered dose is within 10% of the given dose.

4.2. Effect of test dose size on the shape of the dose response curve

Li et al. (2014) in their review paper reported that the saturation of the post-IR IRSL signal is dependent on the experimental conditions applied during the measurement process. For instance Li et al. (2013) and Guo et al. (2015) reported changes to the shape of the dose response curve when using different stimulation temperatures for the post-IR IRSL signal. To explore the impact of changing test dose on the shape of the dose response curve, the luminescence signals from all 300 grains in the second dose recovery experiment (Figs. 4(a) and 5) were summed, to produce a single synthetic aliquot for each test dose. The dose response curves (DRCs) produced from these summed data show a systematic change in shape with the size of the test dose (Fig. 4(b)). The largest change in shape is observed between the lowest test dose (5.1 Gy, ~1% of the given dose, GD) and the 60 Gy (~15% of GD) test dose. Beyond this (i.e. for test doses above 120 Gy, ~30% of GD) the change is limited. The sensitivity normalised signal (L_n/T_n) arising from the 400 Gy given dose when using a 5.1 Gy test dose curve (Fig. 4(b), red square on the y-axis), is close to the maximum L_x/T_x ratio obtained from the regenerated data for the same measurement conditions, and this explains the large number of saturated grains, and the observed underestimation of the mean D_e in Fig. 5(a). Increasing the test dose changes the shape of the DRC, and the 'natural' signal plots below the level of saturation, as seen for the curve built for the 20 Gy test dose (Fig. 4(b), orange) and all larger test doses. However, it is worth noting that for a test dose of 60 Gy or larger all of the DRCs display the same shape and similar L_n/T_n ratios for the natural signals.

D_0 is a convenient measure to characterise the rate of change in curvature of the DRC. D_0 values for the dose response curves in Fig. 4(b) show a general pattern of an increase in D_0 (from 159 ± 87 Gy to 556 ± 66 Gy) as the size of the test dose is increased (from 5 Gy to 320 Gy). The D_0 values for the DRC obtained using the smallest test dose (5 Gy) is less than half the given dose (400 Gy). For quartz, Wintle and Murray (2006) cautioned that when D_e was

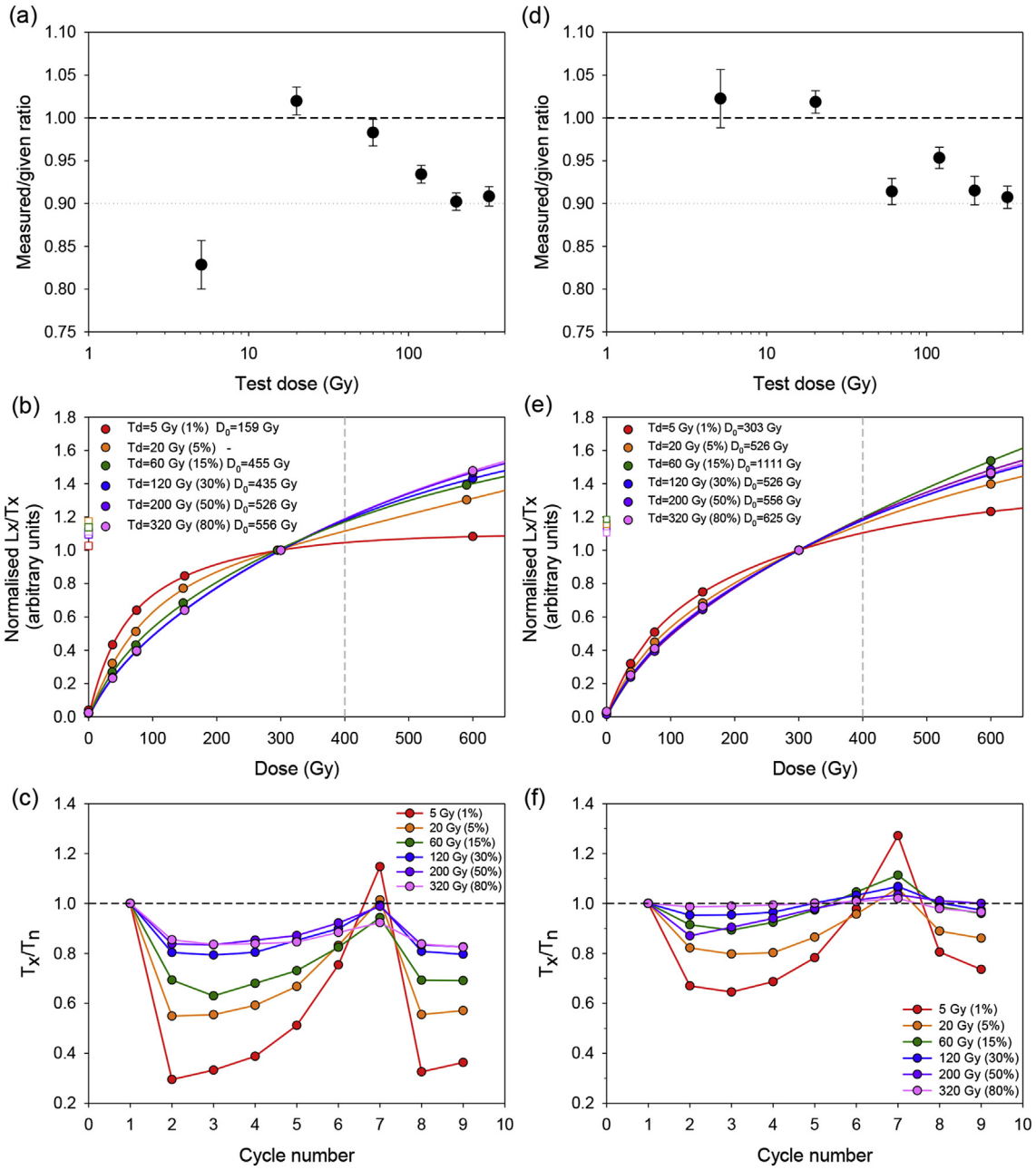

Fig. 4. (a)–(c) Data collected using protocol in Table 1(a). (d)–(f) Data collected using protocol in Table 1(b) which includes an additional 500s IR stimulation after measurement of L_x and T_x. (a, d) Mean measured to given dose ratios (GD ~400 Gy), test dose ranging from ~5 Gy to ~320 Gy. (b, e) Dose response curves (DRC), normalised to the 300 Gy regeneration dose point, for summed post-IR $IRSL_{225}$ data obtained using different test doses (Td). In (b) the D_0 value for a test dose of 20 Gy is ommitted due to difficulty fitting the DRC. The vertical dashed line represents the given dose of 400 Gy. (c, f) Sensitivity change recorded during construction of the DRCs in (b, e).

more than twice the value of D_0 the low slope of the dose response curve at the point where the natural signal is interpolated onto the DRC meant that small uncertainties in the natural measurement (L_n/T_n) would result in large uncertainties in the D_e value; it is likely that similar effects will be seen with feldspars. For feldspars, the change in D_0 with test dose will impact upon the dose range over which the method can be used; for dating older samples it may therefore be advantageous to utilise a larger test dose.

4.3. Effect of test dose size on apparent sensitivity change

The SAR measurement protocol includes a test dose, used to monitor and correct for sensitivity change occurring within the measurement cycle. When measuring the OSL signal from quartz, it is usual to integrate the signal from the start of the OSL decay curve which is dominated by the fast component, and subtract a signal from later in the decay curve to remove the contribution from other components of the OSL signal. Changes in the size of T_x (normally plotted as a ratio to the first measurement of the test dose, T_n) are interpreted as changes in the sensitivity of the sample (that is the intensity of the luminescence signal arising from irradiation), and a variety of different patterns of sensitivity change are observed in quartz (e.g. Armitage et al., 2000).

The change in sensitivity observed for the post-IR $IRSL_{225}$ signal during construction of the dose response curves shown in Fig. 4(b) (where the luminescence signals from 300 grains have been

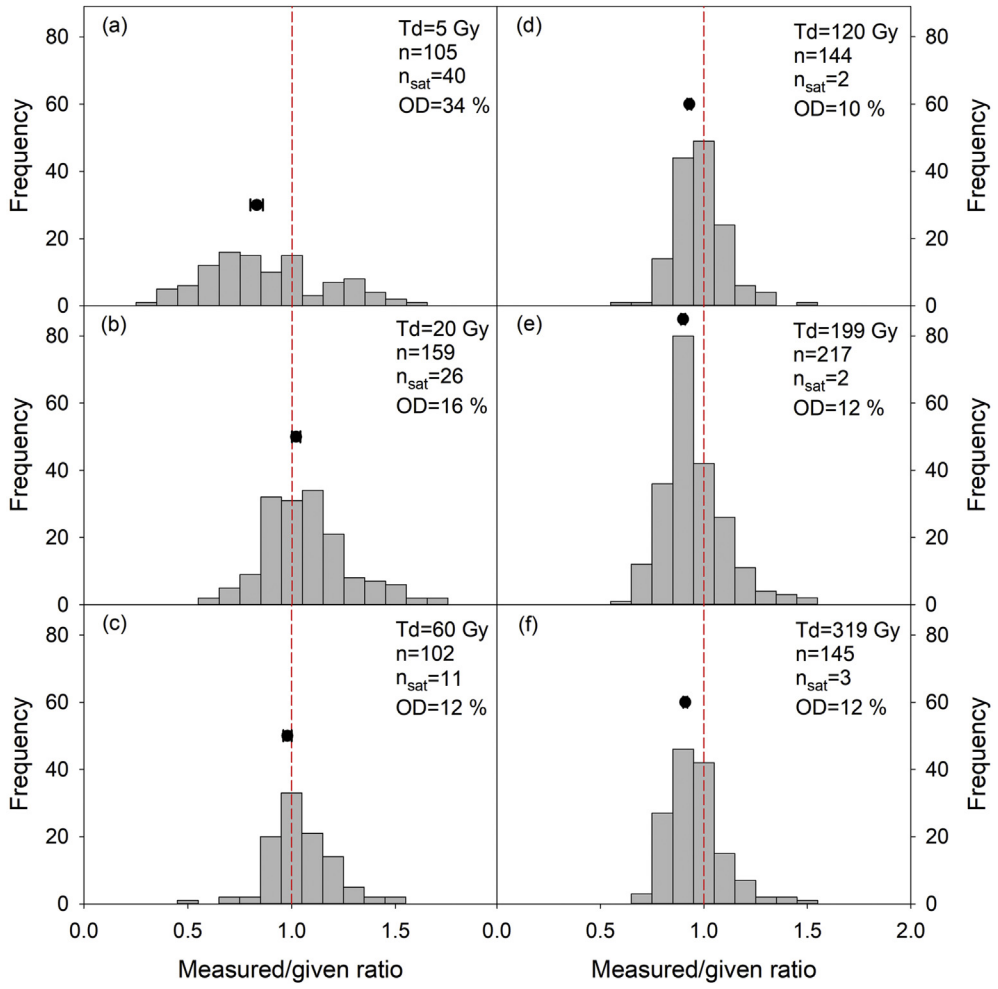

Fig. 5. The measured to given dose ratios for single grains of K-feldspar for the data shown in Fig. 4(a). The mean measured to given dose ratio for the distribution is denoted by the black dot shown with error bars (plotted against an arbitrary y-value). Measurements were made using the post-IR $IRSL_{225}$ protocol with a variable test dose (Td); n represents the number of grains included in the D_e distribution excluding the number of saturated grains (n_{sat}) and the dashed line indicates the given dose normalised to 1. Radial plots of these distributions are included in the supplementary information (Fig. S2).

combined) varies systematically as the size of the test dose is altered (Fig. 4(c)). At small test doses very large sensitivity changes are seen, with T_x decreasing by up to 75% (5 Gy, 1% of GD) (Fig. 4(c)), but as the test dose increases, the maximum amount of sensitivity change decreases to 18% (for a test dose of 320 Gy, 80% of GD). The change in behaviour is most apparent for low test doses, and for test doses of 120 Gy (30% of GD) and above rather little change is seen. The greatest sensitivity change always occurs between cycles 1 and 2 and cycles 7 and 8; these represent the progression from a large regeneration dose (e.g. cycle 1~400 Gy) to a small regeneration dose (e.g. cycle 2 = 0 Gy).

The variation in sensitivity change observed during a SAR sequence when using different test doses (Fig. 4(c)) is consistent with the changes in the shape of the DRC (Fig. 4(b)). For the lowest test dose (5.1 Gy), the value of T_x increases by more than a factor of three as the dose response curve is constructed with increasingly large regeneration doses (cycles 2 to 7 in Fig. 4(c)). The large increase in the size of T_x leads to enhanced curvature of the DRC, while for larger test doses the change in T_x is smaller (a factor of less than 1.4 for a test dose of 320 Gy, Fig. 4(c)), and curvature of the DRC is less (Fig. 4(b)). What is occurring during the SAR protocol to drive these changes in the intensity of T_x?

4.4. Signal transfer between L_x and T_x measurements

Unlike quartz, feldspar does not have a fast component that is rapidly reduced during optical stimulation. The absence of discrete components in the post-IR IRSL signal, and its slow rate of decay under IR stimulation, mean that it is difficult to ensure that the luminescence signal has been reduced to a negligible level before administering further radiation doses. It is common at the end of each cycle in SAR procedures applied to feldspars (Table 1(a), Step 9) to include a step involving optical stimulation, normally at a temperature higher than that used for making the L_x or T_x measurement (e.g. Buylaert et al., 2012; Nian et al., 2012). This is designed to reduce the amount of charge in the sample which remains at the end of the cycle and which would otherwise still be present in the next SAR cycle. A common justification for the inclusion of this step is to reduce recuperation. However, no similar step is normally used to prevent charge from the regeneration dose (Table 1(a), Step 1) still being present when the response to the test dose is measured (T_x: Table 1(a), Step 8).

To explore the relationship between the L_x and T_x measurement, the two signals were compared directly. The L_x and T_x post-IR IRSL decay curves (summed from 300 grains) that were used to

construct Fig. 4(b), were used to obtain the signal intensity in the first channel of the T_x measurement (Table 1(a), Step 8) and to plot this as a function of the intensity of the last channel from the preceding L_x measurement (Table 1(a), Step 4). In a regeneration method, ideally both the L_x and T_x measurements would completely remove the luminescence signal of interest, no excess signal would be carried over into the subsequent measurements, and the data points in Fig. 6(a) would plot along a straight line with a slope approximating zero. However, the data (Fig. 6(a)) show a good correlation, and can be fitted with a linear regression with a positive slope. If signal remaining at the end of the L_x measurement were simply acting as some baseline on top of which charge from the test dose were being added, one might expect the slope of the lines in Fig. 6(a) to be 1.00, or less. However, this is not what is seen. The lowest slope is 2.42, and the slope increases with increasing test dose size. Two possible explanations for the slope being greater than one are (i) that thermal transfer during the preheat of the test dose (Table 1(a), Step 6) is transferring relatively inaccessible charge so that it becomes more easily accessible in the next IR stimulation, or (ii) that the amount of charge remaining in the sample is altering the trapping probability for the subsequent test dose irradiation. However at this stage it is not possible to determine which of these is the cause. What is clear is that the signal remaining from the regeneration dose at the end of the L_x measurement is having a significant impact upon T_x (as seen in Fig. 6(b) and (c)). Fig. 6(a) plots the absolute values from the measurements of L_x and T_x, but what can also be deduced from this diagram and from Fig. 6(b) and (c) is that using a larger test dose reduces the percentage change in T_x as a function of L_x (as already seen in Fig. 4(c)). Whilst the larger test dose masks the impact of L_x, a more elegant solution would be to alter the measurement procedure in order to minimise the charge carried over from L_x to T_x.

5. Extended IR stimulation to reduce carry-over of charge

In Section 4 a large (~400 Gy) given dose was successfully recovered by using a test dose that was between 5 and 80% of the given dose (Fig. 4(a)). However, the data presented in Fig. 6 show a substantial amount of charge being carried over from L_x to the next T_x measurement; since the exact origin of this charge is unclear, the term charge transfer is not used here, and 'carry-over of charge' is used instead. Thus, in this section a protocol is tested which includes an additional 500 s stimulation at 225 °C with IR LEDs after each L_x measurement (Table 1(b), Step 5), designed to minimise the carry-over of charge from L_x to T_x. Additionally, the high temperature (290 °C) IR stimulation after each T_x measurement (Table 1(a), Step 9) was replaced by a 500 s IR LED stimulation at 225 °C, in an attempt to minimise sensitivity change. This new protocol (Table 1(b)) was tested using the same range of test doses as used in Section 4.

Using the modified SAR protocol, the mean measured to given dose ratio (Fig. 4(d)) lies within 10% of unity for all test doses, even 5 Gy (1% of GD) which had previously failed this test (Fig. 4(a)). As anticipated, the inclusion of the additional IR stimulation after measurement of L_x leads to a more muted change in shape of the dose response curve with increasing test dose (Fig. 4(e)) than that seen when using the sequence in Table 1(a) (Fig. 4(b)), and the change in T_x for the different test doses is much reduced (cf Fig. 4(f) and (c)). The D_0 values for the DRCs shown in Fig. 4(d) still broadly increase with test dose (with the exception of the value for a test dose of 60 Gy, which appears anomalous), but the D_0 values (303 ± 35 Gy to 625 ± 146 Gy) are all consistently larger than seen previously (Section 4.2). In contrast with the data in Fig. 4(b), the value of D_0 (303 Gy) for the lowest test dose (5 Gy) is now large enough that the anticipated D_e (400 Gy) is less than twice the value

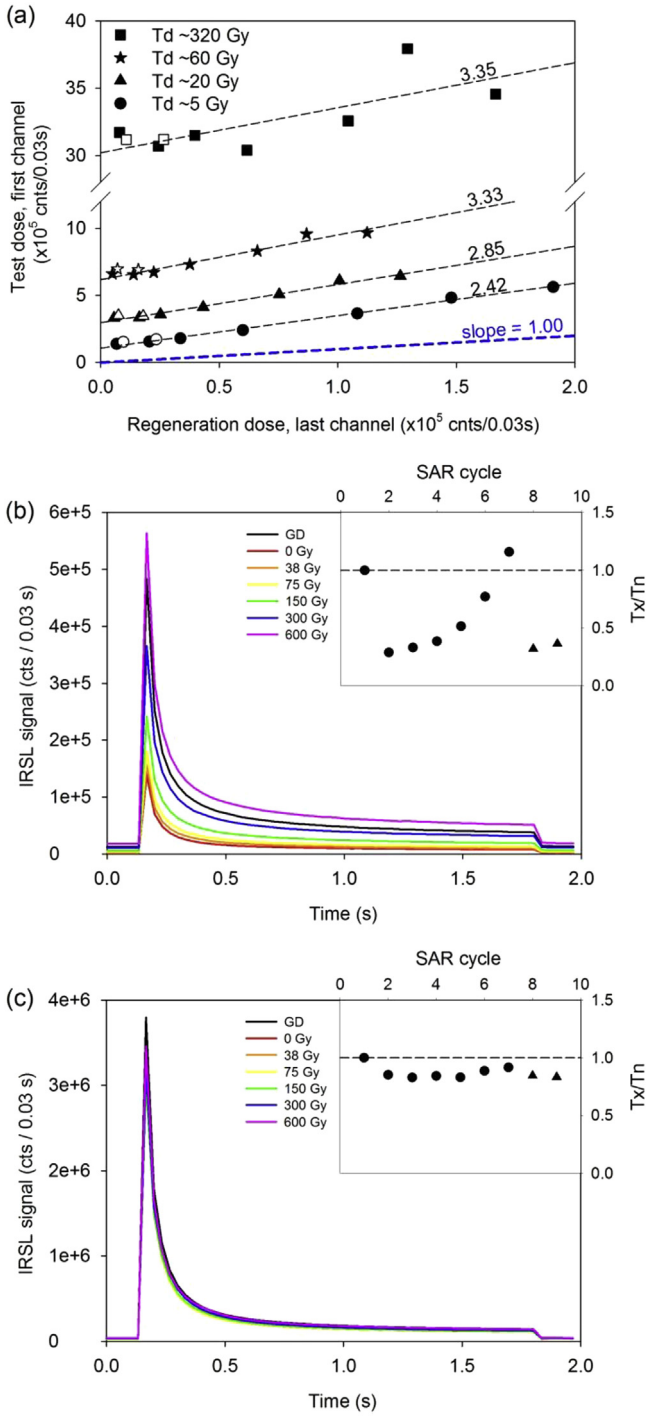

Fig. 6. (a) Assessing the amount of signal carried over from the L_x measurements into the subsequent T_x measurement. For data shown in Fig. 4(a), the first channel of T_x from the IR laser stimulations is plotted as a function of the last channel of the preceding L_x measurement. Data are shown for one summed aliquot (100 grains) for each test dose. Open symbols show data from repeated regeneration doses. Values are shown for the slope of each dashed line, constructed using a linear regression function. (b) The IRSL decay curves (T_x) used in Fig. 6(a) demonstrate the strong dependence of the T_x signal magnitude upon the preceding regeneration dose (given in legend) for the 5 Gy test dose, and (c) the much lower proportionate impact for the 320 Gy test dose.

of D_0. The dose recovery ratio is close to unity (1.02 ± 0.03), and though the single grain data still exhibit substantial overdispersion (OD) of 29% (Fig. S3 and Fig. S4), this value is slightly lower than that

seen previously (34%, Fig. 5(a) and Fig. S2). For the larger test doses (i.e. ≥ 20 Gy, ~5% GD) the values of OD are similar to those seen in Fig. 5(b–f).

Data from Section 4 showed significant carry-over of signal occurring between the L_x measurement and subsequent T_x measurement (Fig. 6(a)), with the slope of the relationship varying from 2.42 to 3.35. In contrast, data obtained using the modified SAR protocol (Table 1(b), Fig. 4(d–f)) shows a much smaller amount of signal carried over between the two measurements (Fig. 7). Linear regressions now have a slope of ~0.3 for all test dose sizes, ten times smaller than for the previous dataset, and are no longer dependent upon the size of the test dose. The fact that the slope of the linear regressions is not zero, implies that there is still a small amount of charge being carried over from the L_x measurement into the T_x measurement, and this may explain the subtle changes in shape of the DRC still seen in Fig. 4(e).

6. Discussion

A key assumption of a single aliquot regeneration method is that the signal being measured is removed completely during measurement, prior to any subsequent irradiation and further measurement (e.g. Duller, 1991; Wallinga et al., 2000, p. 530). This assumption is generally met when SAR is applied to the fast component of quartz. Durcan and Duller (2011) showed that using blue LEDs delivering 30.6 mW cm^{-2} to the sample, the fast component of the quartz OSL signal was calculated to fall to 0.1% of its initial level after just 3.7 s of optical stimulation. The level falls to 0.001% after 6.1 s, and after 40 s stimulation (the period commonly used in SAR measurements), the fast component is calculated to be 2×10^{-33} times smaller than its initial level (Fig. S5(a)). The fast component of quartz can be relatively simply isolated by integrating the early part of the OSL signal and subtracting a background from later in the OSL decay curve where only the medium and slow components remain. In contrast, the IRSL signal from feldspars decays much more slowly than the fast component of the quartz OSL signal, and follows a power law (e.g. Bailiff and Poolton, 1991; Huntley, 2006; Pagonis et al., 2012) instead of a simple exponential decay (Fig. S5(b)). Furthermore, the IRSL signal is not composed of discrete components, meaning that subtraction of a signal derived from later in the decay curve does not result in the isolation of a single rapidly bleached component as it does in quartz. The function of the background subtraction that is universally applied when using SAR for feldspars is unclear, and its inclusion is probably a spurious hangover from the application of SAR to quartz. The IRSL signal rarely reaches a stable low level at the end of measurements of the regeneration dose or test dose (e.g. Li et al., 2013), and using a fixed period of time for IR measurement is likely to result in different signal intensities at the end of each regeneration measurement. Duller (1991) recognised the difficulty of removing the IRSL signal from feldspars in the first paper describing single aliquot methods of equivalent dose determination. He described a method where the IR stimulation of a sample continued for as long as was required to reduce the IRSL signal to below a preset threshold (in his case 600 cps). Whilst this approach reduced the change in apparent sensitivity that was observed, it did not remove it entirely, and hence the method was abandoned. The only method that appears to be effective at removing the signal is to undertake IRSL measurements at higher temperatures. Thus the use of a high temperature IRSL measurement (e.g. at 325 °C) at the end of each SAR cycle (e.g. Buylaert et al., 2012) is effective at reducing the post-IR $IRSL_{290}$ signal as demonstrated by the low recuperation values measured. However, inserting this type of treatment between the measurement of L_x and administration of the test dose risks leading to sensitivity change that could not be corrected for using a standard SAR approach. Indeed, undertaking a dose recovery experiment using the post-IR $IRSL_{225}$ protocol, with a 5 Gy test dose and an additional IRSL stimulation at 290 °C after each L_x and T_x measurement, resulted in a measured to given dose ratio of 1.29 ± 0.03.

Figs. 6 and 7 confirm that for the measurement parameters used in this study, the assumption that the IRSL signal is removed during each measurement is not met (and it is probably not met in the majority of measurements of feldspar IRSL using SAR). One of the most significant impacts of charge remaining from one dose upon the measurement of the luminescence signal arising from the next dose is to make it appear as if the sample is changing its luminescence sensitivity (e.g. Fig. 4(c) and (f)). In turn, this change in apparent sensitivity leads to changes in the shape of the dose response curve (Fig. 4(b) and (e)). However, the signal measured as T_x no longer originates solely from the test dose, but contains charge resulting from the regeneration dose as well (as shown by Figs. 6 and 7). Thus T_x is not a measure of sensitivity, but a complex mixture resulting from both the regeneration dose and test dose; using it to correct the dose response curve may lead to inaccuracies. Since the amount of charge carried over from the regeneration dose to the measurement of the test dose response is closely coupled with the size of the regeneration dose (Figs. 6(a) and 7(a)), this

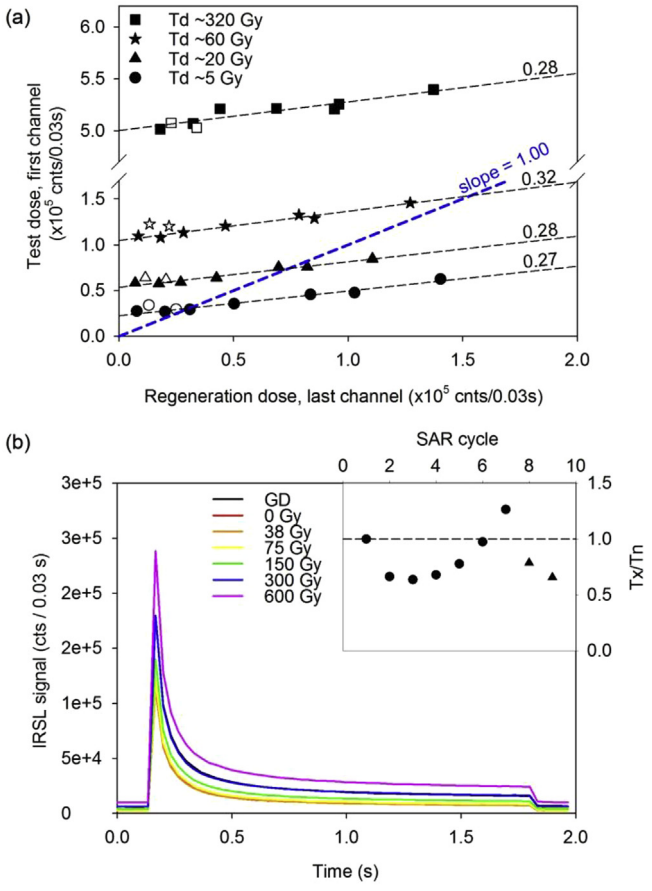

Fig. 7. (a) Quantifying the amount of signal carry-over between the L_x and T_x measurements by directly comparing the last channel of L_x with the first channel of T_x from the IR laser stimulations for data shown in Fig. 4(d). The additional IR stimulation after both L_x and T_x measurements has reduced the signal difference by a factor of 10 (see Fig. 6(a)). Data presented are for one synthetic aliquot. Open symbols show data from repeated regeneration doses. Values are shown for the slope of each dashed line, constructed using a linear regression function. (b) IRSL decay curves (T_x) for the 5 Gy test dose used to construct Fig. 7 (a). Note the smaller variation in T_x intensity as a function of regeneration dose compared with that seen in Fig. 6(b).

error in sensitivity correction will not be detected by a recycling test, and may only weakly be seen in the dose recovery ratio. Thus the tests used for assessing the validity of the SAR protocol are not effective as quality assurance checks for feldspar. The addition of a second measurement of the IRSL signal at 225 °C (Table 1(b), Step 5) after measuring L_x reduced, but did not remove entirely, the dependence of the test dose signal (T_x) on the regeneration signal (cf. Fig. 7(a and b) with Fig. 6(a and b)).

The single aliquot regenerative (SAR) dose method, developed at the end of the 1990's and into the early 2000's for use with the optically stimulated luminescence (OSL) signal from quartz (Murray and Wintle, 2000; Wintle and Murray, 2006), has been adopted for use with the luminescence signals from feldspars (e.g. Wallinga et al., 2000; Buylaert et al., 2012). Few modifications have been made to the SAR method in order to tailor the method to this different mineral. In hindsight this is perhaps surprising, especially given that there is a general consensus that SAR applied to quartz is most effective when a dominant fast component exists in the OSL signal (Wintle and Murray, 2006), whilst the IRSL and post-IR IRSL feldspar signals are thought not to contain distinct components (Thomsen et al., 2011; Pagonis et al., 2012).

Large changes in overdispersion in D_e values from single grains were observed depending upon the size of the test dose used (e.g. Figs. 3 and 5). It is not clear whether these changes in overdispersion are primarily the result of changes in the apparent D_0 of the dose response curve, leading to many grains being close to, or beyond, the limit of saturation, or whether the overdispersion arises from grain-to-grain variability in the extent to which charge is carried over from the regeneration dose to the test dose measurement. Analyses of the type shown in Figs. 6 and 7 at a single grain level have not revealed any systematic relationship between slope and the ability to recover a dose, but further analysis would be helpful. Regardless of the exact cause of the changes in overdispersion, its existence is important when considering the application of single grain IRSL measurements to dating.

7. Conclusions

A prerequisite for the successful application of the SAR protocol is the ability to reduce the luminescence signal to a negligible level after each measurement in order to accurately correct for sensitivity change. Thus, it has become common practise to include a high temperature clean out at the end of each step to remove trapped charge prior to each L_x measurement; unfortunately this does not prevent the carry-over of charge from the L_x measurement into the T_x measurement. A series of dose recovery experiments showed that the feldspar IRSL signal is not reduced to background levels after IR stimulation, which results in a carry-over of charge from the L_x measurement into the T_x measurement, ultimately leading to inaccuracies in sensitivity correction and DRC construction. The effect of signal transfer during the post-IR IRSL measurement protocol was dealt with in two ways in this study. First, its impact was reduced by applying a large test dose thereby decreasing the relative size of the charge carried over. Second, the magnitude of the carried-over charge was reduced by including an additional IR stimulation at the same second stimulation temperature after both the L_x and T_x measurements. Both approaches were shown to be equally effective at recovering a known given dose (Fig. 4(a) and (d)) and reducing apparent sensitivity change (Fig. 4(c) and (f)). However, the latter approach also minimises potential thermally induced sensitivity change due to high temperature thermal treatments, such as the high temperature clean out at the end of each step. A convenient way of assessing whether charge carry-over is significant is by the comparison of test dose signals through the SAR sequence (e.g. Fig. 6(b), (c) and 7(b)).

The lack of a rapidly-depleted feldspar luminescence signal results in the signal not being reduced to low enough levels after each measurement to ensure accurate sensitivity correction. Future SAR-type procedures for measurement of feldspars should aim to minimise the impact of the regeneration dose upon the measurement of the test dose, thus making T_x a more accurate measure of sensitivity.

Acknowledgements

This research was conducted whilst DC was in receipt of a Doctoral Career Development Scholarship funded by Aberystwyth University. Luminescence work was supported by an NERC grant (CC003) to GATD and HMR. DC's doctoral research into South African environments has also been supported by the Geological Society of South Africa (GSSA) Research, Education and Investment Fund, the Quaternary Research Association (QRA) New Research Workers' Award and the British Society for Geomorphology (BSG) Postgraduate Research Grant. The authors would like to thank Dr Richard Lyons for providing sample Aber162/MPT4 for use in this research, Hollie Wynne for laboratory support, Jakob Wallinga and another anonymous reviewer for their constructive comments which improved this paper and Ian Bailiff for editorial handling.

Appendix A. Supplementary data

Supplementary data related to this article can be found at http://dx.doi.org/10.1016/j.radmeas.2017.07.005.

References

Armitage, S.J., Duller, G.A.T., Wintle, A.G., 2000. Quartz from southern Africa: sensitivity changes as a result of thermal pretreatment. Rad. Meas. 32, 571–577.
Bailiff, I.K., Poolton, N.R.J., 1991. Studies of charge transfer mechanisms in feldspars. Nucl. Tracks Rad. Meas. 18, 111–118.
Bøtter-Jensen, L., Andersen, C.E., Duller, G.A.T., Murray, A.S., 2003. Developments in radiation, stimulation and observation facilities in luminescence measurements. Rad. Meas. 37, 535–541.
Buylaert, J.-P., Murray, A.S., Thomsen, K.J., Jain, M., 2009. Testing the potential of an elevated temperature IRSL signal from K-feldspar. Rad. Meas 44, 560–565.
Buylaert, J.-P., Jain, M., Murray, A.S., Thomsen, K.J., Thiel, C., Sohbati, R., 2012. A robust feldspar luminescence dating method for Middle and Late Pleistocene sediments. Boreas 41, 435–451.
Buylaert, J.P., Murray, A.S., Gebhardt, A.C., Sohbati, R., Ohlendorf, C., Thiel, C., Wastegård, S., Zolitschka, B., 2013. Luminescence dating of the PASADO core 5022-1D from Laguna Potrok Aike (Argentina) using IRSL signals from feldspar. Quat. Sci. Rev. 71, 70–80.
Buylaert, J.-P., Yeo, E.-Y., Thiel, C., Yi, S., Stevens, T., Thompson, W., Frechen, M., Murray, A., Lu, H., 2015. A detailed post-IR IRSL chronology for the last interglacial soil at the Jingbian loess site (northern China). Quat. Geochron 30, 194–199.
Colarossi, D., Duller, G.A.T., Roberts, H.M., Tooth, S., Lyons, R., 2015. Comparison of paired quartz OSL and feldspar post-IR IRSL dose distributions in poorly bleached fluvial sediments from South Africa. Quat. Geochron 30, 233–238.
Duller, G.A.T., 1991. Equivalent dose determination using single aliquots. Nucl. Tracks Rad. Meas. 18, 371–378.
Duller, G.A.T., 1992. Luminescence Chronology of Raised Marine Terraces, Southwest North Island, New Zealand. Unpublished PhD thesis. University of Wales, Aberystwyth.
Duller, G.A.T., 2015. The Analyst software package for luminescence data: overview and recent improvements. Anc. TL 33, 35–42.
Durcan, J.A., Duller, G.A.T., 2011. The fast ratio: a rapid measure for testing the dominance of the fast component in the initial OSL signal from quartz. Rad. Meas. 46, 1065–1072.
Fu, X., Li, S.-H., Li, B., 2015. Optical dating of aeolian and fluvial sediments in north Tian Shan range, China: luminescence characteristics and methodological aspects. Quat. Geochron 30, 161–167.
Huntley, D.J., 2006. An explanation of the power-law decay of luminescence. J. Phys. Cond. Mat. 18, 1359–1365.
Guo, Y.-J., Li, B., Zhang, J.-F., Roberts, R.G., 2015. Luminescence-based chronologies for Palaeolithic sites in the Nihewan Basin, northern China: First tests using newly developed optical dating procedures for potassium feldspar grains. J. Archaeol. Sci.: Rep. 3, 31–40.
Jain, M., Ankjærgaard, C., 2011. Towards a non-fading signal in feldspar: insight into charge transport and tunnelling from time-resolved optically stimulated

luminescence. Rad. Meas. 46, 292–309.
Kars, R.H., Reimann, T., Wallinga, J., 2014. Are feldspar SAR protocols appropriate for post-IR IRSL dating? Quat. Geochron 22, 126–136.
Li, B., Jacobs, Z., Roberts, R., Li, S.-H., 2014. Review and assessment of the potential of post-IR IRSL dating methods to circumvent the problem of anomalous fading in feldspar luminescence. Geochron 41, 178–201.
Li, B., Li, S.H., 2011. Luminescence dating of K-feldspar from sediments: a protocol without anomalous fading correction. Quat. Geochron 6, 468–479.
Li, B., Roberts, R.G., Jacobs, Z., 2013. On the dose dependency of the bleachable and non-bleachable components of IRSL from K-feldspar: improved procedures for luminescence dating of Quaternary sediments. Quat. Geochron 17, 1–13.
Murray, A.S., Wintle, A.G., 2000. Luminescence dating of quartz using an improved single-aliquot regenerative-dose protocol. Rad. Meas. 32, 57–73.
Nian, X., Bailey, R.M., Zhou, L., 2012. Investigations of the post-IR IRSL protocol applied to single K-feldspar grains from fluvial sediment samples. Rad. Meas. 47, 703–709.
Pagonis, V., Jain, M., Murray, A.S., Ankjærgaard, C., Chen, R., 2012. Modelling of the shape of infrared stimulated luminescence signals in feldspars. Rad. Meas. 47, 870–876.
Qin, J.T., Zhou, L.P., 2012. Effects of thermally transferred signals in the post-IR IRSL SAR protocol. Rad. Meas. 47, 710–715.
Reimann, T., Thomsen, K.J., Jain, M., Murray, A.S., Frechen, M., 2012. Single-grain dating of young sediments using the pIRIR signal from feldspar. Quat. Geochron 11, 28–41.
Sohbati, R., Murray, A.S., Buylaert, J.-P., Ortuño, M., Cunha, P.P., Masana, E., 2012. Luminescence dating of Pleistocene alluvial sediments affected by the Alhama de Murcia fault (eastern Betics, Spain) – a comparison between OSL, IRSL and post-IRIRSL ages. Boreas 41, 250–262.
Thomsen, K.J., Murray, A.S., Jain, M., Bøtter-Jensen, L., 2008. Laboratory fading rates of various luminescence signals from feldspar-rich sediment extracts. Rad. Meas. 43, 1474–1486.
Thomsen, K.J., Murray, A.S., Buylaert, J.P., Jain, M., Hansen, J.H., Aubry, T., 2016. Testing single-grain quartz OSL methods using sediment samples with independent age control from the Bordes-Fitte rockshelter (Roches d'Abilly site, Central France). Quat. Geochron 31, 77–96.
Thomsen, K.J., Murray, A.S., Jain, M., 2011. Stability of IRSL signals from sedimentary K-feldspar samples. Geochron 38, 1–13.
Trauerstein, M., Lowick, S.E., Preusser, F., Schlunegger, F., 2014. Small aliquot and single grain IRSL and post-IR IRSL dating of fluvial and alluvial sediments from the Pativilca valley. Peru. Quat. Geochron 22, 163–174.
Wallinga, J., Murray, A.S., Wintle, A.G., 2000. The single-aliquot regenerative-dose (SAR) protocol applied to coarse-grain feldspar. Rad. Meas. 32, 529–533.
Wintle, A.G., 1973. Anomalous fading of thermoluminescence in mineral samples. Nature 245, 143–144.
Wintle, A.G., Murray, A.S., 2006. A review of quartz optically stimulated luminescence characteristics and their relevance in single aliquot regeneration dating protocols. Rad. Meas. 41, 369–391.
Yi, S., Buylaert, J.-P., Murray, A.S., Thiel, C., Zeng, L., Lu, H., 2015. High resolution OSL and post-IR IRSL dating of the last interglacial-glacial cycle at the Sanbahuo loess site (northeastern China). Quat. Geochron 30, 200–206.
Yi, S., Buylaert, J.-P., Murray, A.S., Lu, H., Thiel, C., Zeng, L., 2016. A detailed post-IR IRSL dating study of the Niuyangzigou loess site in northeastern China. Boreas 45, 644–657.